ICSV19
Vilnius, Lithuania
July 08-12, 2012

WHEN WILL A FLAME DESCRIBING FUNCTION APPROACH TO THERMOACOUSTICS WORK WELL?

Simon J. Illingworth and Matthew P. Juniper

Department of Engineering, University of Cambridge, UK, e-mail: si250@cam.ac.uk

In any thermoacoustic analysis, it is important not only to predict linear frequencies and growth rates, but also the amplitude and frequencies of any limit cycles. The Flame Describing Function (FDF) approach is a quasi-linear analysis which allows the prediction of both the linear and nonlinear behaviour of a thermoacoustic system. This means that one can predict linear growth rates and frequencies, and also the amplitudes and frequencies of any limit cycles. The FDF achieves this by assuming that the acoustics are linear and that the flame, which is the only nonlinear element in the thermoacoustic system, can be adequately described by considering only its response at the frequency at which it is forced. Therefore any harmonics generated by the flame's nonlinear response are not considered. This implies that these nonlinear harmonics are small or that they are sufficiently filtered out by the linear dynamics of the system (the low-pass filter assumption). In this paper, a flame model with a simple saturation nonlinearity is coupled to simple duct acoustics, and the success of the FDF in predicting limit cycles is studied over a range of flame positions and acoustic damping parameters. Although these two parameters affect only the linear acoustics and not the nonlinear flame dynamics, they determine the validity of the low-pass filter assumption made in applying the flame describing function approach. Their importance is highlighted by studying the level of success of an FDF-based analysis as they are varied. This is achieved by comparing the FDF's prediction of limit-cycle amplitudes to the amplitudes seen in time domain simulations.

1. Introduction

Thermoacoustic oscillations can occur whenever combustion takes place inside an acoustic resonator. Unsteady combustion is an efficient acoustic source [1], and combustors tend to be highly resonant systems. Therefore for suitable phase between unsteady combustion and acoustic perturbations, large-amplitude self-excited oscillations can occur. Gas turbines, aeroengine afterburners, ramjets, boilers and furnaces are all susceptible to combustion oscillations. Combustion oscillations are of particular concern for the new generation of gas turbines operating under lean premixed prevaporized (LPP) conditions. LPP combustion reduces emissions of oxides of Nitrogen (NO_x), but is especially prone to combustion oscillations [2].

The importance of predicting thermoacoustic oscillations is therefore clear. In any thermoacoustic analysis, it is important not only to predict linear frequencies and growth rates, but also the amplitude and frequencies of any limit cycles. The Flame Describing Function (FDF) approach is a quasi-linear analysis which allows the prediction of both the linear and nonlinear behaviour of a thermoacoustic system. This means that one can predict linear growth rates and frequencies, and also the amplitudes and frequencies of any limit cycles. It was first applied to thermoacoustics analytically

by Dowling [3, 4], and later applied to an experimental set-up by Noiray et al. [5]. Both sets of studies were able to predict limit cycle amplitudes and frequencies with good success. It is important to understand, then, if this will always be the case, or if there are situations under which the FDF does not perform well. That question is the focus of this paper.

2. The describing function approach

The describing function (DF) approach was first developed in the 1950s by researchers in the fields of circuits and feedback control. It is a method to predict the amplitude and frequency of limit-cycle oscillations in nonlinear feedback systems, and is applicable to systems which involve a nonlinear process in feedback with a linear process. The describing function approach treats the nonlinear element in a quasi-linear manner: for sinusoidal forcing at the input of the nonlinearity, the DF retains only the response of the nonlinearity at this frequency. Any higher frequencies (harmonics) or lower frequencies (subharmonics) generated by the nonlinearity are discarded.

One circumstance under which the DF approach will work well, therefore, is when any harmonics generated by the nonlinearity are small. This might be the case for certain nonlinearities, but is certainly not true in general. Let us take the "ideal relay" nonlinearity as an example. This nonlinearity is commonly encountered in electrical circuits, the field in which the DF approach was first developed. The ideal relay nonlinearity generates a third harmonic which is one third as large as the fundamental, which is certainly not small. (The second harmonic and all other even harmonics are zero.)

Another circumstance under which the DF approach will work well, which is more likely in practice, is when the linear part of the feedback system filters out any higher harmonics generated by the nonlinear part. This is often referred to as the low-pass filtering assumption. It is central to the success of the DF approach, since it ensures that any nonlinearity output harmonics are filtered to the extent that only a trivial quantity is fed back to the nonlinearity input [6].

For many engineering systems this low-pass filtering assumption is well-justified, the linear dynamics providing sufficient low-pass filtering that higher harmonics may be ignored. In a thermoacoustic system the acoustics typically constitute the linear element, which means that the low-pass filter assumption may not be justified in all cases. For simple duct acoustics, for example, the acoustic duct modes are at frequencies $\omega, 2\omega, 3\omega$, and so on. Therefore any nonlinear harmonics generated by a flame forced at frequency ω will be at precisely the frequencies of the higher acoustic modes.

3. Thermoacoustic modeling

The purpose of this paper is to understand under what conditions a describing function approach will work well for predicting the nonlinear behaviour of a thermoacoustic system. To do so we couple a simple nonlinear flame model to simple acoustics in a one-dimensional duct.

3.1 Acoustics

Acoustic perturbations are considered on top of the mean velocity in the duct. The perturbations are governed by the (non-dimensional) momentum and energy equations:

$$\frac{\partial u}{\partial t} + \frac{\partial p}{\partial x} = 0; \quad \frac{\partial p}{\partial t} + \frac{\partial u}{\partial x} + \xi p = \beta\, \delta_f(x - x_f)\, q, \tag{1}$$

where $\beta = (\gamma - 1)\, \tilde{Q} \,/\, (\gamma\, \tilde{p}\, \tilde{u})$, which we will call the coupling parameter. The acoustic time- and length-scales, t, x are non-dimensionalized using the speed of sound and the duct length. u and p are the non-dimensional perturbations in velocity and pressure. (The pressure has been non-dimensionalized using γM.) δ_f is the Dirac delta function, and ξ represents acoustic damping. For

the simple geometry considered (see Fig. 2), $\partial u/\partial x$ and p are both set to zero at the ends of the duct. These boundary conditions are enforced by choosing basis sets that match them:

$$u(x,t) = \sum_{j=1}^{N} u_j(t)\cos(j\pi x); \quad p(x,t) = \sum_{j=1}^{N} p_j(t)\sin(j\pi x). \tag{2}$$

(For the momentum equation to be satisfied, $u_j(t)$ and $p_j(t)$ must be related by $p_j(t) = \dot{u}_j(t)/j\pi$.) The acoustic damping, ξ, is treated by assigning a damping parameter, ζ_j, to each mode:

$$\xi_j = 2\zeta_j\omega_j, \quad \text{with } \zeta_j = c_1 j + c_2 j^{-1/2}. \tag{3}$$

This model is based on correlations developed by Matveev [7] from models in Landau and Lifshitz [8]. The Galerkin discretization of Eq. (2) leads to a state-space model relating the perturbation in heat release rate, $q(t)$, to the acoustic velocity perturbation at the flame, $u_f(t)$:

$$\dot{x}(t) = A\,x(t) + \beta\,B\,q(t) \tag{4a}$$
$$u_f(t) = C\,x(t), \tag{4b}$$

where x is the column vector $x = [u_{1,..,N}; p_{1,..,N}]$ and A, B, C are suitably-dimensioned matrices. The coupling parameter β remains a variable in Eq. (4a) to make clear that it enters linearly into the acoustic equations.

In § 5 we will make use of the transfer function corresponding to Eq. (4). This is provided by taking Laplace transforms of Eq. (4) to give the transfer function for the full acoustic state, $A(s)$; and by substituting Eq. (4a) into Eq. (4b) to give the transfer function for the velocity at the flame, $A_f(s)$:

$$A(s) = \frac{x(s)}{q(s)} = \beta\,(sI - A)^{-1}B, \tag{5a}$$
$$A_f(s) = \frac{u_f(s)}{q(s)} = \beta\,C(sI - A)^{-1}B, \tag{5b}$$

where s is the Laplace variable. Clearly the two transfer functions are related by $A_f(s) = CA(s)$.

Let us consider the effect of the flame position, x_f on these two transfer functions. Since the B matrix is in part composed of the sine basis functions, then by Eq. (5a) the unsteady heat release rate, $q(t)$, cannot excite acoustic mode j directly whenever $\sin(j\pi x_f) = 0$. Therefore if the flame position is such that $\sin(j\pi x_f) = 0$, then acoustic mode j is zero for all time. Similarly, since the C matrix is in part composed of the cosine basis functions, then by Eq. (5b) the contribution of mode j to the velocity at the flame position, u_f, is zero whenever $\cos(j\pi x_f) = 0$. This simply corresponds to mode j having a velocity node at x_f. To summarize: for zero initial condition, the velocity and pressure (and therefore energy) of mode j will be zero for all time if x_f is such that $\sin(j\pi x_f) = 0$. The velocity at the flame, u_f, contributed by mode j will be zero whenever $\sin(j\pi x_f)\cos(j\pi x_f) = 0$, which happens either when mode j is zero, or when a node in the velocity prevents mode j being observed at x_f. These two considerations will be important in understanding the results in § 5.[1]

3.2 Flame

To model the unsteady flame dynamics, the flame response is divided into two parts: a linear flame model, which completely characterizes the flame response for small perturbations; and a non-linear model, which ensures that the flame response is bounded for large perturbations (and which is responsible for the generation of nonlinear harmonics).

[1] The situation is not quite this simple. A more complete analysis would require consideration of the observability and controllability Gramians of the state-space model (Eq. 4) – but the same results hold when one does so.

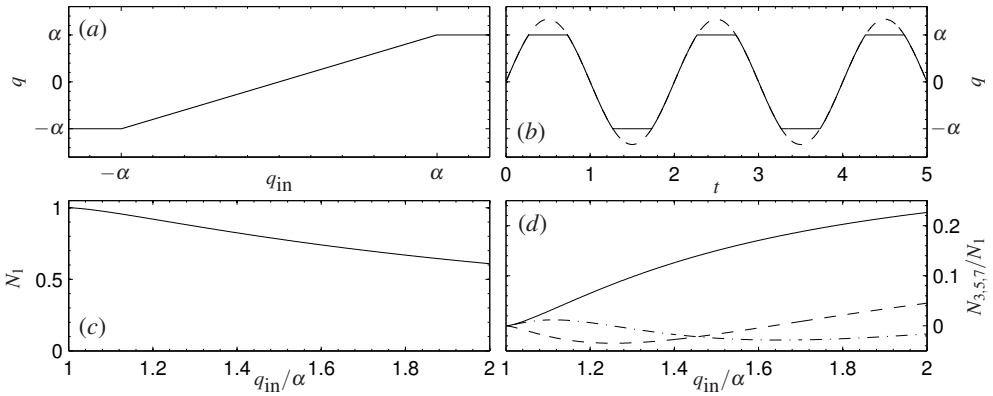

Figure 1. The nonlinear flame model. The form of the nonlinearity is shown in (*a*), and a typical time signal that it gives rise to is shown in (*b*). The describing function of the saturation nonlinearity is shown in (*c*), while (*d*) shows the sizes of the 3rd (—); the 5th (- -); and the 7th (-·-) nonlinear harmonics.

The linear flame model used is the same as that adopted by Dowling [3], which was derived from the empirical flame model of Bloxsidge et al. [9]. The equation relating the unsteady heat release rate, $q(t)$, to the unsteady velocity at the flame, $u_f(t)$, is

$$\left(\tau_1 \frac{d}{dt} + 1\right)\left(\tau_2 \frac{d}{dt} + 1\right) q(t) = u_f(t - \tau_d). \tag{6}$$

Taking Laplace transforms of Eq. (6) gives the flame transfer function,

$$F(s) = \frac{q(s)}{u_f(s)} = \frac{1}{(\tau_1 s + 1)(\tau_2 s + 1)} e^{-s\tau_d}. \tag{7}$$

This model, while simple, captures the salient features of the unsteady flame response; the gain is unity at low frequencies; the gain decreases with increasing frequency (which is governed by the two time constants τ_1, τ_2); and the unsteady heat release responds to unsteady velocity fluctuations after some time delay, τ_d.

For nonlinear fluctuations, we continue to use Eq. (6), but assume that the unsteady heat release rate never exceeds some ratio, α, of the steady-state heat release rate. Therefore for large fluctuations, the heat release rate saturates at the value α, as shown in Fig. 1 (*a*, *b*). This nonlinear saturation model of the flame is similar to that used by Dowling [3]. (Note, however, that in Dowling, the saturation occurs *before* the linear flame dynamics (Eq. 7) are applied, while in our case the saturation occurs *afterwards* – see Fig. 2.)

Figure 1 (*c*, *d*) characterizes this nonlinear flame model, both in terms of its describing function, N_1, and in terms of its generation of higher harmonics, $N_{3,5,7}$. Notice that, because the nonlinearity is odd, the even-numbered higher harmonics ($N_{2,4,6,..}$) are all zero. Therefore if the first acoustic mode excites the flame, for example, then the flame will not in turn excite the second mode, the fourth mode, and so on.

3.3 Coupled thermoacoustic system

The feedback interconnection of the acoustics of § 3.1 and the flame of § 3.2 gives the overall, coupled thermoacoustic system, which is shown in Fig. 2. Two outputs are shown, in keeping with the parameters of interest that will be studied in § 5: the velocity at the flame, $u_f(t)$; and the total instantaneous acoustic energy, $E(t)$. In § 5 we will consider the total acoustic energy integrated over one cycle of the fundamental acoustic mode, which is constant in a limit-cycle and given by

$$E_c = \int_0^{\frac{2\pi}{\omega_1}} E(t)\, dt = \int_0^{\frac{2\pi}{\omega_1}} \frac{1}{4}\, x^T(t)\, x(t)\, dt. \tag{8}$$

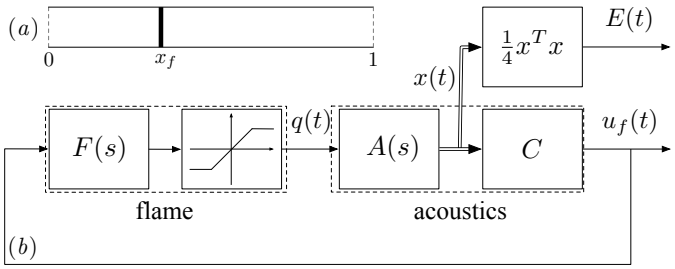

Figure 2. The thermoacoustic system: (*a*) the duct geometry with a typical flame position; and (*b*) a block diagram of the coupled thermoacoustic system which is useful for a describing function analysis. Both the acoustic velocity at the flame, u_f, and the total instantaneous acoustic energy, $E(t)$, are shown as outputs.

4. Ensuring linear instability

We study the success of the describing function approach as two parameters are varied: the modal acoustic damping, ζ_j; and the position of the flame in the duct, x_f. We vary these in order to change the relative contribution of the higher acoustic modes. However, we wish to retain linear instability (with the same frequency and growth rate) in the first mode as we do so. Clearly, varying these two parameters will not only affect the dynamics of the higher acoustic modes, but also the dynamics of the first acoustic mode which we want to remain constant. In this section we first describe the effect produced by changes in the modal damping and the flame position. We then explain how variations in the coupling parameter, β and in the flame time delay, τ_d can be used to ensure linear instability of the first acoustic mode (with a given frequency and growth rate) even as ζ_j and x_f are varied.

4.1 Varying the modal damping, ζ_j

Clearly, reducing the damping of a given acoustic mode will increase its propensity for excitation by unsteady heat release. Recall that the modal damping is given by (Eq. 3)

$$\zeta_j = c_1 j + c_2 j^{-1/2}. \tag{9}$$

We would like the damping of the first acoustic mode, $\zeta_1 = c_1 + c_2$, to remain constant, and we do this by fixing the value of $(c_1 + c_2)$. We would like to vary the damping of the higher acoustic modes, and we can do this by varying the *relative* sizes of c_1 and c_2. Since we expect the third acoustic mode to have the greatest influence among the higher modes, the parameter that we vary is the ratio ζ_3/ζ_1:

$$\frac{\zeta_3}{\zeta_1} = \frac{3\,c_1 + 3^{-1/2} c_2}{c_1 + c_2}. \tag{10}$$

Having fixed $(c_1 + c_2)$ and ζ_3/ζ_1, we can solve Eq. (10) for c_1 and c_2.

4.2 Varying the flame position, x_f

For the simple duct acoustics considered, changing the position of the flame has two effects, as discussed in § 3.1. First, x_f determines (via the $\sin j\pi x_f$ terms) the extent to which the unsteady heat release can excite acoustic mode j. Second, x_f determines (via the $\cos j\pi x_f$ terms) the extent to which acoustic mode j is observed in the velocity at the flame, u_f.

4.3 Fixing the frequency and growth rate of the unstable mode

For linear fluctuations we may ignore the saturation block in Fig. 2. Then the *linear* transfer function between a disturbance entering the flame and the resulting velocity at the flame is

$$P(s) = \frac{F(s)A_f(s)}{1 - F(s)A_f(s)}, \tag{11}$$

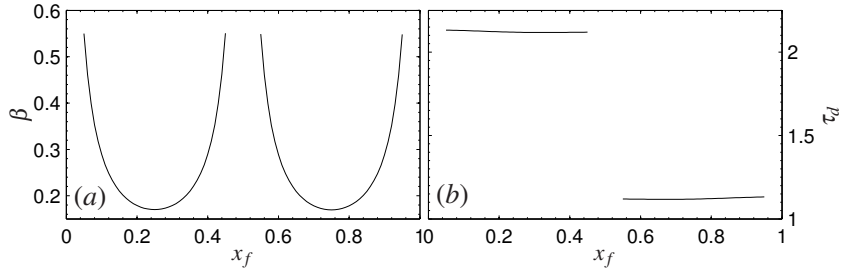

Figure 3. The required variations in (*a*) β and (*b*) τ_d to ensure linear instability of the first acoustic mode (with the same frequency and growth rate) as the flame position is varied.

where the linear flame transfer function, $F(s)$, is given by Eq. (7), and the acoustic transfer function for the velocity at the flame, $A_f(s)$, is given by Eq. (5b). The eigenvalues of this coupled thermoacoustic system are those points in the complex s-plane where the denominator of Eq. (11) vanishes: that is, when

$$F(s)A_f(s) = 1. \tag{12}$$

We can isolate the acoustic gain, β, and the flame's time delay, τ_d by defining another transfer function, $L(s)$, such that $\beta L(s)e^{-s\tau} = F(s)A_f(s)$. We do this so that we can see how we must vary β and τ_d to achieve a certain eigenvalue of the coupled system. If we require an eigenvalue at $s = \sigma + i\omega$, then clearly we require that

$$\beta L(\sigma + i\omega)e^{-(\sigma+i\omega)\tau} = 1 + i0. \tag{13}$$

The real and imaginary parts of Eq. (13) can each be solved to give the β and τ_d required. $L(\sigma + i\omega)$ varies with the modal damping and the flame position, and therefore so must β and τ_d if Eq. (13) is to be satisfied.

Figure 3 shows the variation of β and τ_d as the flame position is varied between $0.05 \leq x_f \leq 0.45$ and $0.55 \leq x_f \leq 0.95$, which represents the range of x_f to be studied in § 5. (Since the damping of the first mode, ζ_1, is fixed, β and τ_d remain constant with changes in ζ_3/ζ_1.) The value of β required becomes very large near the centre and at the ends of the tube. This is because $\sin(\pi x_f)$ is small here, so a large β is required for the flame to excite the first acoustic mode sufficiently for instability. The value of τ_d remains almost constant for each half of the duct. The large difference in the required τ_d for the two halves is caused by the change in sign of the first mode shape across $x_f = 0.5$: the flame's time delay must counteract this change in phase.

5. Results and discussion

The FDF predictions of thermoacoustic limit cycles for different flame positions and different damping parameters are shown in Fig. 4 – both for three acoustic modes and for twenty acoustic modes ($N = 3, 20$ in Eq. 2). The flame position is varied between $0.05 \leq x_f \leq 0.45$ and $0.55 \leq x_f \leq 0.95$ in increments of 0.01, and the damping ratio is varied between $1.0 \leq \zeta_3/\zeta_1 \leq 3.0$ in increments of 0.5. The left-hand half of Fig. 4 is concerned with the peak velocity at the flame, which we denote u_f^p. The right-hand half is concerned with the total acoustic energy in the duct integrated over one cycle of the fundamental frequency, E_c, which was introduced in Eq. (8). In both halves of the figure, the upper four plots directly compare the prediction given by the FDF to that found in time domain simulations, while the lower four plots show the normalized discrepancy between them.

5.1 Peak velocity fluctuation at the flame

Let us first consider the FDF prediction of the peak velocity at the flame, u_f^p, for three acoustic modes. Figure 4 (*a*) compares the FDF prediction of the peak velocity to that found in time domain

simulations for three acoustic modes, and Fig. 4 (*b*) shows the normalized discrepancy between them. The FDF prediction of the velocity is very nearly constant in each half of the duct. This is because it is based on the dynamics of the coupled system (Fig. 2) at the frequency of the instability, which is the frequency of the first acoustic mode. Since β and τ_d are varied to ensure the same (unstable) dynamics of the first mode, the FDF prediction remains constant. Notice, however, that the FDF prediction is not quite symmetric about the duct's centre. This is caused by the change in the time delay across $x_f = 0.5$: the solution of Eq. (13) tells us that a change in τ_d necessitates a small change in β to recover the same eigenvalue, and a change in β in turn affects the FDF prediction.

The peak velocity seen in time domain simulations, meanwhile, varies with the flame position, and the variation is largest when the damping of the third mode is smallest. The time domain solution is also nearly symmetric about the duct centre. This is because all even harmonics generated by the flame are zero. (The slight asymmetry is for the same reason given above.) As discussed in § 3.1, an important parameter for the contribution of mode j to the velocity at the flame is $\sin(j\pi x_f)\cos(j\pi x_f)$. This term simultaneously accounts for the level of excitation of mode j by the flame ($\sin j\pi x_f$); and for its velocity mode shape ($\cos j\pi x_f$). To be able to assign a size to this term, we must consider it in relation to the first acoustic mode (which is the source of the instability). Therefore for the third acoustic mode, the parameter of interest is:

$$\frac{\sin(3\pi x_f)\cos(3\pi x_f)}{\sin(\pi x_f)\cos(\pi x_f)}. \tag{14}$$

Equation (14) does not capture the whole picture. In particular, it does not account for the fact that the third acoustic mode, once excited, will in turn perturb the flame. Nevertheless, the family of curves seen in Fig. 4 (*b*) is well-described by Eq. (14).

Let us now consider the twenty mode case, which is shown in Fig. 4 (*c*, *d*). The results are qualitatively very similar to the three mode case, and quantitatively only small differences are seen. This suggests that the higher acoustic modes are much less excited by the flame's nonlinear harmonics, and this is to be expected given their higher damping. It is interesting that the discrepancy between the FDF and time domain solutions can be made both larger and smaller by the inclusion of the higher acoustic modes, depending on the position of the flame. This is simply because the superposition of the higher modes can be both constructive and destructive.

5.2 Total acoustic energy over one cycle

Figures 4 (*e*, *g*) show the total acoustic energy integrated over one cycle of the first acoustic mode, again for both three and twenty acoustic modes. The large variation in the total acoustic energy with changing flame position is caused by the velocity mode shape. For self-sustained oscillations to occur, the acoustic gain between unsteady heat release and the velocity seen at the flame must be sufficiently large. Since the ends of the duct correspond to maxima in the mode shape, the amplitude of the first mode need only be relatively small to ensure a sufficiently large gain here. The centre of the duct, however, corresponds to a node of the velocity mode shape. Therefore the required amplitude of the first mode increases as $x_f \to 0.5$.

Figures 4 (*f*, *h*) show the normalized discrepancy between the FDF prediction of the acoustic energy and that found in time domain simulations. The normalized discrepancy is always very small, with a maximum value of approximately 0.5 %. This is because the amplitude of each acoustic mode is squared (Eq. 8), and therefore the vast majority of the acoustic energy is in the first acoustic mode. Unlike the peak velocity, where the discrepancy was well-described by considering the relative size of the third acoustic mode, the discrepancy in the acoustic energy is caused by two effects, whose contributions are of similar sizes: (i) that the FDF neglects any energy in the higher modes; and (ii) that the FDF's prediction of the fundamental mode itself is in error. A full explanation requires consideration of both of these contributions, which length constraints of this paper does not permit.

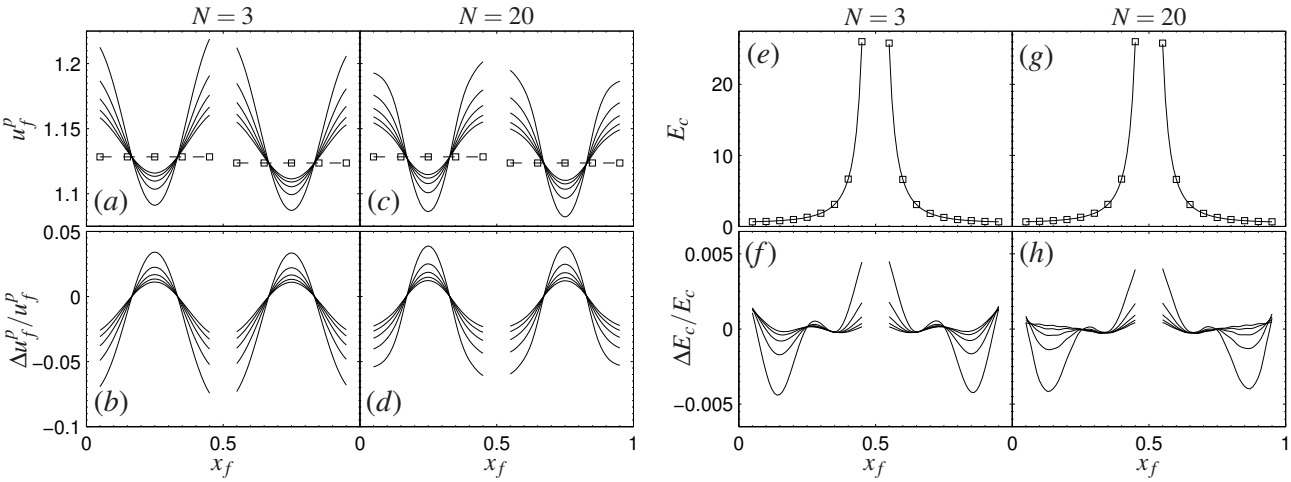

Figure 4. The FDF prediction of the acoustic velocity at the flame (left four figures), and of the total acoustic energy over one cycle (right four figures). The comparison with time domain simulations is made for three acoustic modes in (a,b,e,f) and for 20 acoustic modes in (c,d,g,h). The top row compares the time domain data (—) to the FDF prediction (–□–). The bottom row shows the normalized discrepancy between them. For a given x_f, the discrepancy is greatest for the smallest damping ratio of $\zeta_3/\zeta_1 = 1$.

6. Conclusions

The success of the flame describing function (FDF) approach for predicting thermoacoustic limit cycles has been studied by considering a simple nonlinear flame model coupled to simple duct acoustics. The FDF approach performs well in all of the cases studied, predicting the peak velocity at the flame to within 7.0 % in all cases, and predicting the total acoustic energy over one cycle to within 0.5 % in all cases. The results suggest that the FDF can perform well even when the contribution of higher acoustic modes is significant. We must remember, however, that in these results all even nonlinear harmonics are zero, and so nonlinear excitation of the second acoustic mode is not possible. It would be interesting, therefore, to consider nonlinearities which are not odd, and to investigate the influence of the flame's even nonlinear harmonics.

References

[1] A. P. Dowling, J. E. Ffowcs Williams, Sound and Sources of Sound, Ellis Horwood, 1983.

[2] G. A. Richards, M. C. Janus, Characterization of oscillations during premix gas turbine combustion, J. Eng. Gas Turbines Power 120 (2) (1998) 294–302.

[3] A. P. Dowling, Nonlinear self-excited oscillations of a ducted flame, J. Fluid Mech. 346 (1997) 271–290.

[4] A. P. Dowling, A kinematic model of a ducted flame, J. Fluid Mech. 394 (1999) 51–72.

[5] N. Noiray, D. Durox, T. Schuller, S. Candel, A unified framework for nonlinear combustion instability analysis based on the flame describing function, J. Fluid Mech. 615 (1) (2008) 139–167.

[6] A. Gelb, W. E. Vander Velde, Multiple-input describing functions and nonlinear system design, McGraw-Hill, New York, 1968.

[7] K. Matveev, Thermoacoustic instabilities in the Rijke tube: experiments and modeling, Ph.D. thesis, California Institute of Technology, 2003.

[8] L. D. Landau, E. M. Lifshitz, Fluid Mechanics, Pergamon Press, 1959.

[9] G. J. Bloxsidge, A. P. Dowling, P. J. Langhorne, Reheat buzz: an acoustically coupled combustion instability. Part 2. Theory, J. Fluid Mech. 193 (1) (1988) 445–473.